

# Introducing Sunshine Forecast to Improve On-Board Energy Management of Hybrid Solar Vehicles

G.Rizzo\*, M.Sorrentino\*

\*Dept. Of Mechanical Engineering, University of Salerno, 84084 Fisciano (SA), Italy

Email: grizzo – msorrentino @unisa.it

**Abstract:** Management strategies of Hybrid Solar Vehicles differ from Hybrid Electric Vehicles, which usually adopt charge sustaining strategies, because the battery can be recharged also during parking time by solar energy. Therefore, at the end of driving the final state of charge (SOC) is required to be low enough to allow full storage of solar energy captured in the next parking phase, whereas the adoption of an unnecessary constantly-low value of final SOC would give additional energy losses and compromise battery lifetime. The effects of different strategies of selection of final SOC are studied by simulation over hourly solar data at different months, and the benefits achievable by estimating the energy expected in next parking phase are assessed.

**Keywords:** Hybrid Vehicles, Solar Energy, Energy Management.

## 1. INTRODUCTION

In last years an increasing attention is being paid to the integration of Hybrid Electric Vehicles (HEV) and Photo-Voltaic (PV) sources (Letendre et al., 2003), as confirmed by the recent launch of an HEV mounting solar panels by a major automotive company. Hybrid Solar Vehicles (HSV) can give substantial benefits to fuel economy and emissions, especially in the case of intermittent use in urban driving (Arsie et al., 2007, 2008). Moreover, their economic feasibility may be achieved in a near future, also thanks to the decreasing cost (Fig. 1) and to the increasing efficiency of photovoltaic panels, as shown by the results of optimal design analysis considering both energy, weight and costs involved (Arsie et al., 2007).

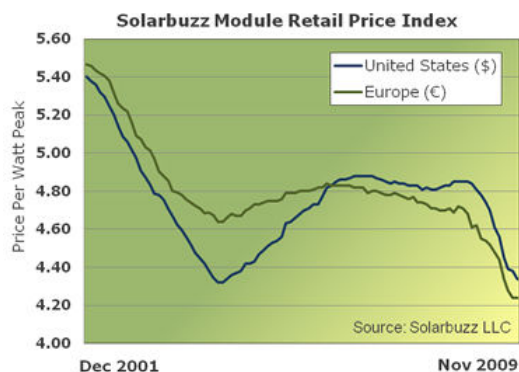


Fig. 1 – Trends in photovoltaic panels price.

A prototype of HSV with series structure has been developed (Fig. 2), and significant research work on HSV has been done in last years by the authors and their colleagues at the University of Salerno. Studies are also in course to estimate the benefits obtainable with a moving solar roof with self-

orienting capabilities, to maximize the energy captured during parking phases (Coraggio et al., 2010).



Fig. 2 – The prototype of Hybrid Solar Vehicle.

It has been evidenced that the energy management of these vehicles, in spite of many similarities of HSV's with HEV's, could not simply borrowed from the solutions developed for HEV: in fact, while in these latter a charge sustaining strategy is usually adopted, in HSV's the battery can be recharged also during parking time by solar energy, and therefore a charge depletion strategy has to be followed during driving, as it happens for Plug-In Hybrid Electric Vehicles (PHEV) (Marano et al., 2009). Anyway, there are again some important differences between PHEV and HSV: while for PHEV the recharge is mainly finalized to extend the vehicle range, for HSV's the input energy is free, and solar recharge should be maximized not only to extend the range, but mainly to minimize fuel consumption and CO<sub>2</sub> emissions. Therefore, at the end of driving cycle the final state of charge (SOC) should be sufficiently low to leave room for the solar

energy to be stored in the battery in the next parking phase. On the other hand, the adoption of an unnecessary low value of final SOC could produce additional energy losses associated to battery operation, so increasing fuel consumption.

In the paper, the effects of different strategies of selection of final SOC are studied by simulation over hourly solar data at different months and locations, and the benefits achievable by estimating the energy expected in next parking phase are assessed. The simulations are carried out with a dynamic model of an HSV previously developed (Arsie et al., 2007; Arsie et al., 2010), including a rule-based energy management strategy described in next chapters. A solar calculator, based on the analysis of time series of solar radiation over about 30 years, has been used [[www.nrel.gov/rredc/pywatts](http://www.nrel.gov/rredc/pywatts)] to estimate the hourly solar energy achievable at different locations and months on a solar roof in horizontal position.

## 2. RULE-BASED ENERGY MANAGEMENT OF A SERIES HYBRID SOLAR VEHICLE

Differently than HEV, HSV requires a day-through charge sustaining strategy to avoid wasting solar energy during parking phases (Arsie et al., 2007). The authors themselves have recently proposed an on-line implementable Rule-Based (RB) control policy to address such a goal accounting for the effects of operating variables on fuel consumption and SOC, including thermal transient effects related to engine start and stop, as well as expected daily insolation (Rizzo et al., 2009). It has been shown that the fuel consumption obtained by this implementable strategy is very close to the benchmark obtained in off-line by Genetic Algorithms (Sorrentino et al., 2009; Sorrentino et al., 2010; Arsie et al., 2009).

Specifically in this work, the RB strategy was modified so as to incorporate perfect solar prediction to enhance battery management in driving phases.

The RB control architecture consists of two tasks, external and internal, respectively:

- external task: defines the desired final state of charge  $SOC_f$  (see Figure 3), to be reached at the end of the driving cycle to enable full storage of solar energy captured during the following parking phase.
- internal task: estimates the average power delivered by the ICE-EG (i.e., Internal Combustion Engine – Electric Generator group) and SOC deviation ( $\Delta SOC$ ) from  $SOC_f$  as function of average traction power  $\bar{P}_{tr}$ .

Figure 3 provides a qualitative description of the start&stop strategy enabled by the above-described control tasks. For sake of simplicity, in Figure 3 it is assumed that initial state of charge  $SOC_0$  equals  $SOC_f$  and does not vary with time. The described control strategy relies, on one hand, on the online estimation of current SOC level and, on the other, on predicting or properly estimating average traction power demand over an assigned driving route. Regarding the last point, Rizzo et al. (2009) showed that an a-posteriori (i.e.

based on past data) estimation of  $\bar{P}_{tr}$  ensures good performance of the internal control task. Therefore, a-posteriori estimation was selected here to enhance real-time implementation of the proposed RB strategy. Another important aspect concerns the time window ( $t_h$ ) in which  $\bar{P}_{tr}$  has to be evaluated. Sorrentino et al. (2009) showed that optimal  $t_h$  increases with average traction power. Particularly, for the ECE-EUDC cycle, it was found that optimal  $t_h$  sets at 1091 s, which is the value assumed in the simulation analyses described in section 3.

The next subsections will provide detailed description of the methodologies followed to establish the heuristic rules, as well as analyze rules impact on intermittent ICE operation in a series HSV.

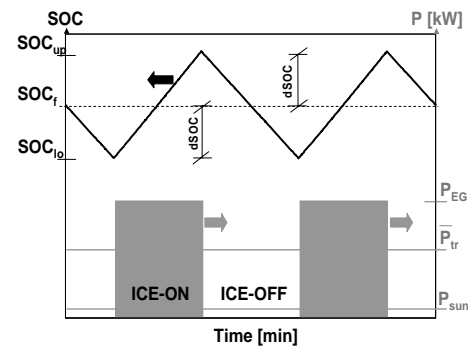


Fig. 3. Schematic representation of the rule-based control strategy for quasi-optimal energy management of a series HSV powertrain.

### 2.1 External task rule

Differently than the previous approach (Rizzo et al., 2009), the target  $SOC_f$  here is estimated as function of effective solar energy to be captured during the next parking phase. Therefore, assuming a perfect prevision of solar energy is available, the external task rule (i.e. Rule 1) will read as:

$$SOC_f = 0.95 - \Delta SOC_p \quad (1)$$

under the constraint:

$$0.15 < SOC_f < 0.7 \quad (2)$$

Where  $\Delta SOC_p$  is the SOC increase due to PV charging during parking phases. In Eq. (1)  $\Delta SOC_p$  is estimated by simulating battery charging during the parking phase, as shown on Figure 4. Regarding parking time estimation, it was calculated assuming: i) solar irradiation, in the selected location (i.e., Los Angeles), lasts for about 10 hours a day on average; ii) daily use of passenger cars is fairly equal to 1.5 hours (Andrè et al., 1999).

Figure 5 shows the impact played by  $\Delta SOC_p$  on optimal  $SOC_f$ . It can be noted that the upper constraint expressed by Eq. (2) introduces a saturation on optimal  $SOC_f$  in correspondence of low solar contribution. Such a choice is justified considering that battery internal resistances reach their minimum around SOC=0.7 (Sorrentino et al., 2010), thus

there is no reason to further increase  $SOC_f$ . In the results section, the importance of correctly estimating  $SOC_f$  depending on effective solar contribution during parking clearly emerges.

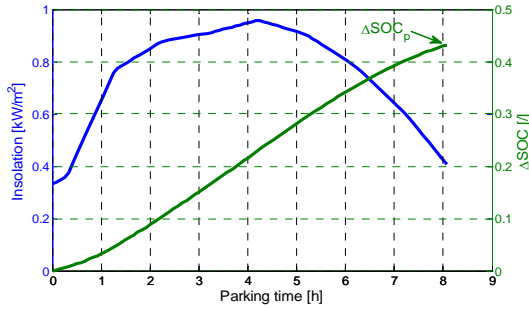


Fig. 4. Evaluation of expected SOC increase due to PV charging during parking phases. PV panel horizontal area and efficiency are assumed equal to 3 m<sup>2</sup> and 0.19, respectively.

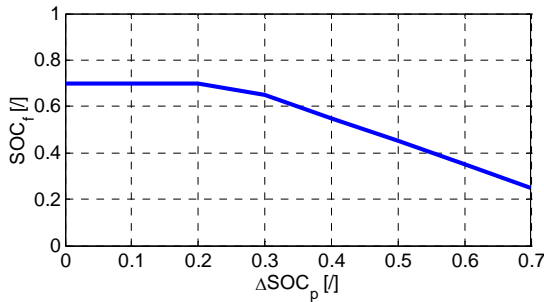


Fig. 5. SOCf variation as function of  $\Delta SOC_p$  (see Eq. 1).

## 2.2 Internal task rules

The details about the following Rule 2 (i.e. Eq. 3) and Rule 3 (i.e. Eq. 4) determination can be found in (Rizzo et al., 2009):

$$P_{EG} = f(\bar{P}_{tr}) \quad (3)$$

$$dSOC = f(\bar{P}_{tr}) \quad (4)$$

Figure 6 compares the  $P_{EG}$  trajectory addressed by Rule 2 with the most efficient ICE-EG operating point ( $P_{EG,opt}$ ), corresponding to about half nominal power (see vehicle specifications in Table 1). Such comparison indicates that at high road loads, Rule 2 exhibits a load following behavior, whereas at low power demand Rule 2 always undergoes  $P_{EG,opt}$ . The latter observation can be explained by analyzing the battery charging phase in case of  $\bar{P}_{tr} = 7$  (see Figure 7).

With Rule 2, a lower charging power is attained as compared to  $P_{EG,opt}$ , thus reducing battery internal losses, on one hand, and ensuring safer operation (Buchmann, 2009) on the other.

It is worth noting, in Figure 7, that the ICE-EG intermittent strategy results in letting the battery meet the whole traction power demand until a lower SOC threshold is reached (Rizzo et al., 2009). Then, since the objective is to restore the initial state of charge, the ICE-EG is turned on at a power level that ensures recharging the battery before driving phase ends.

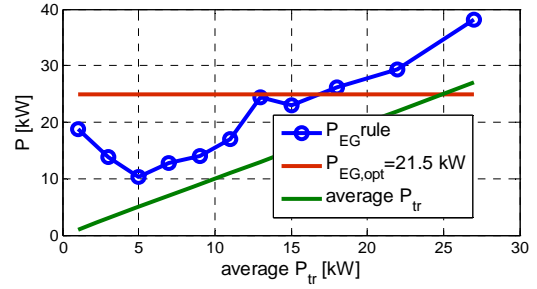


Fig. 6. Comparison between power levels of most efficient ICE-EG operating point and Rule 2.

Figures 8 and 9 show the impact of internal task rules on fuel economies for different driving cycles. It can be seen that both rules, but especially Rule 2, allow achieving significant fuel savings with respect to constant-values-operation of the ICE-EG.

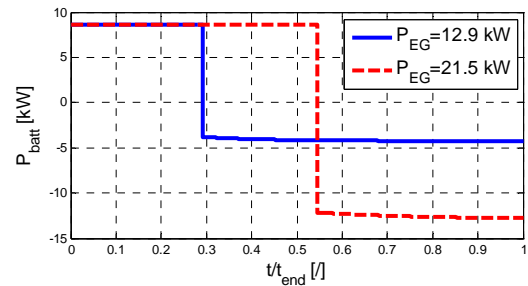


Fig. 7. Transient Battery power when  $\bar{P}_{tr}$  constantly equals 7 kW;  $t$  is current time, whereas  $t_{end}$  is the driving end time.

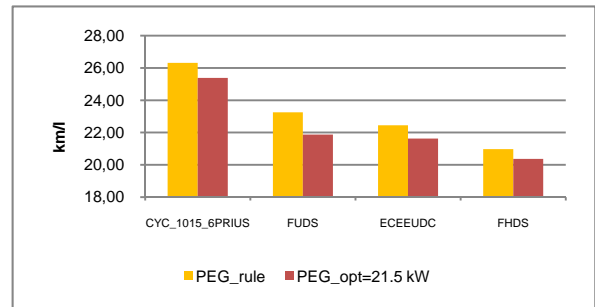


Fig. 8. Impact of Rule 2 on HSV fuel economy.

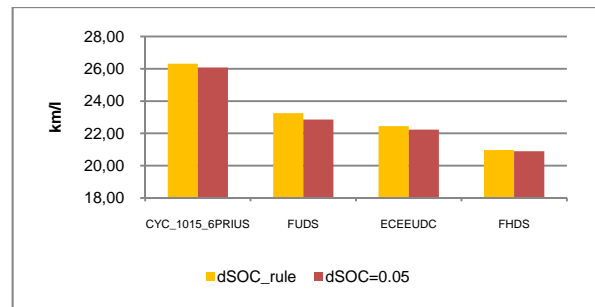


Fig. 9. Impact of Rule 3 on HSV fuel economy.

### 3. RESULTS

In order to assess the benefits associated to the introduction of insolation forecast, a simulation based scenario analysis was carried out. The selected location was Los Angeles, while solar insolation data refer to 1988. Table I and Figure 10 describe, respectively, vehicle specification and a schematic of a typical daily simulation. Regarding this latter point, it is worth remarking here that the knowledge of drive planning is of limited relevance, as the external and internal task (see section 2) are mainly affected by expected (or forecasted) solar insolation and traction power demand, respectively.

In the analysis, restricted to January and July 1988, the external task rule (i.e. Rule 1) was initially deactivated to assess the impact of  $SOC_f$  on fuel consumptions. Three different scenarios were analyzed, with increasing values of the PV efficiency  $\eta_{PV}$ :

Scenario 1:  $\eta_{PV}=0.13$ .

Scenario 2:  $\eta_{PV}=0.19$ .

Scenario 3:  $\eta_{PV}=0.25$ .

While the lower efficiency value is near to most of current polycrystalline PV modules, scenario 2 utilizes high efficiency PV already available on the market, while the value of 0.25 could be reached in a mid-term scenario, according to actual trends and projections.

Table 1. HSV specifications.

Nominal ICE-EG power [kW]	43
Nominal EM power [kW]	90
Number of Lead-acid battery modules	21
Battery capacity $C_B$ [kWh]	6.3
PV horizontal surface [m <sup>2</sup> ]	3
Coefficient of drag (Cd)	0.33
Frontal area [m <sup>2</sup> ]	2.3
Rolling resistance coefficient [l]	0.01
Weight [kg]	1434

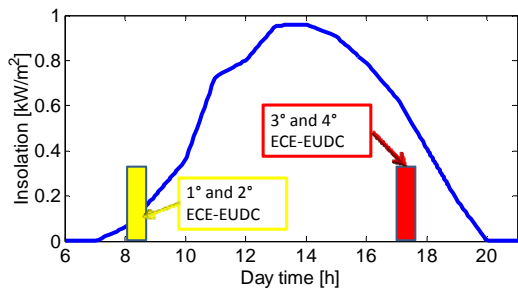


Fig. 10. Schematic representation of a generic daily simulation. Solar insolation trajectory refers to July 13<sup>th</sup> 1988.

Figures 11 through 13 show variation of overall fuel consumption as function of  $SOC_f$ . As expected, the most significant benefits associated to solar energy correspond to

July. For all scenarios, a minimum occurs whose value depends of course on  $\eta_{PV}$ . As  $\eta_{PV}$  increases,  $SOC_f$  must be reduced so as not to waste solar energy during parking phases. Regarding this latter aspect, Figure 12 and Figure 13 interestingly show that adopting  $SOC_f$  constantly equal to 0.7 (most efficient battery operation) causes fuel consumption to significantly increase in July, as appreciable waste of energy occurs during parking phases due to battery saturation.

Figures 11, 12 and 13 also show fuel consumption simulated by introducing insolation forecast, i.e. by activating Rule 1 (i.e. corresponding abscissa is labeled “Rule 1”). As expected, insolation forecast allows better using the battery pack, which in turn results in improved fuel economy. Particularly, Figure 14 indicates that at the end of the 4<sup>th</sup> ECE-EUDC cycle (see Figure 10) Rule 1 addresses  $SOC_f$  around 0.7, whereas the best parametric result obtained for Scenario 2 corresponds to 0.5. This way, Rule 1 imposes that the next ECE-EUDC will start from an optimal battery initial condition, thus resulting in lower battery losses as compared to  $SOC_f=0.5$ . Moreover, Rule 1 ensures battery is kept charged overnight, thus satisfactorily addressing the requirements in term of prolonged battery life (Buchmann, 2009). The latter aspect is widely recognized as highly strategic to enhance both technical and economical feasibility not only for HSV, but for HEV in general.

An overview on fuel economy improvements achievable by insolation forecast is given in Table 2. Once again it can be seen how Rule 1 always allows operating the battery around its optimal condition (i.e. SOC = 0.7 on average). On the other hand, as  $\eta_{PV}$  increases, average SOC simulated in the best parametric case tends to drift from optimal SOC. The latter consideration explains why Rule 1 positively impacts also on January fuel economies, despite the lower solar contribution during winter time. As expected,  $\eta_{PV}$  increase results in larger fuel economy gains achievable by means of insolation forecast as compared to constant  $SOC_f$  operation.

Finally, Figure 15 describes global simulation results attained in Scenario 2 when Rule 1 was activated.

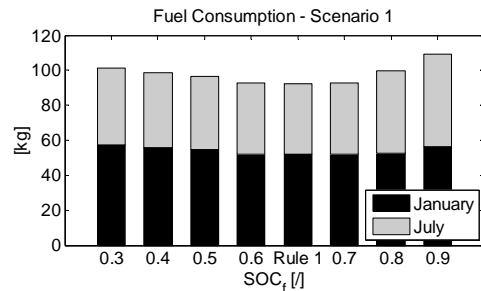


Fig. 11. Simulated Fuel Consumptions for Scenario 1.

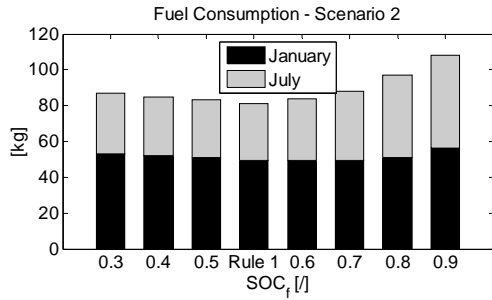


Fig. 12. Simulated Fuel Consumptions for Scenario 2.

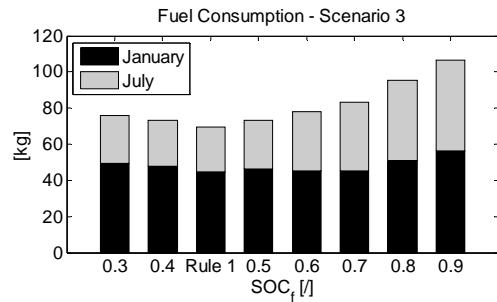


Fig. 13. Simulated Fuel Consumptions for Scenario 3.

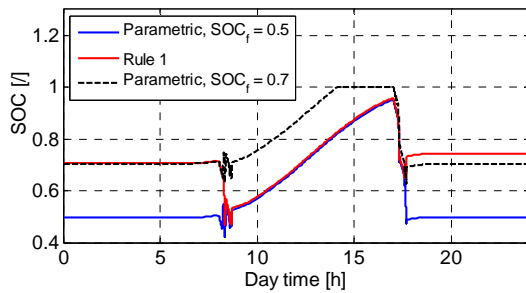


Fig. 14. SOC trajectories simulated for Scenario 2 on July the 13<sup>th</sup> 1988.

Table 2. Overall resume of the scenario analysis outcomes.

	Scenario 1		Scenario 2		Scenario 3	
	Best parametric	Rule 1	Best parametric	Rule 1	Best parametric	Rule 1
[km/l] Jan	20.55	20.55	20.98	21.69	22.29	23.80
[km/l] Jul	26.04	26.59	32.81	33.25	42.50	43.21
Average SOC - Jan	0.62	0.72	0.53	0.73	0.45	0.74
Average SOC - Jul	0.66	0.74	0.61	0.7	0.58	0.69

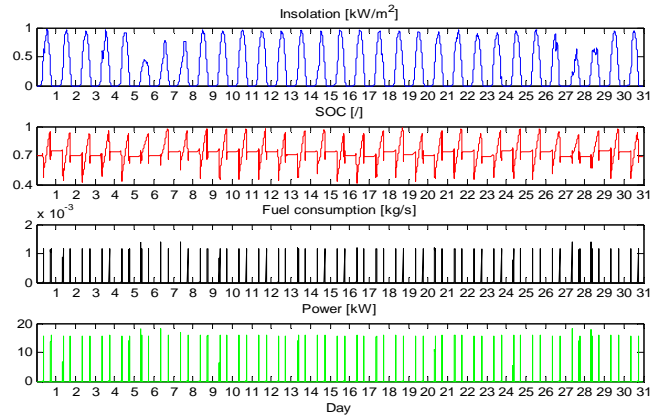


Fig. 15. Global simulation of July 1988. Scenario 2 optimal case with insolation prediction (i.e. Rule 1 activated).

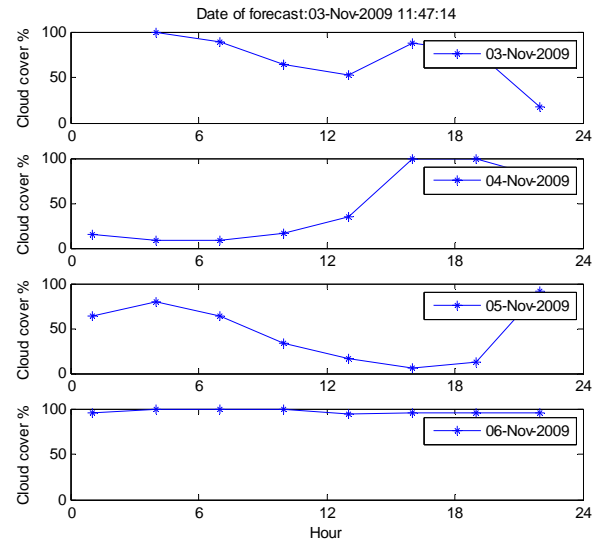


Fig. 16. Cloud cover forecast for Fisciano, Italy.

#### 4. CONCLUSIONS

In order to maximize the benefits obtainable with Hybrid Solar Vehicles, the optimum compromise between two potentially conflicting aspects should be realized: i) to leave as much as possible room in the battery for solar recharge and ii) operate in a favorable battery SOC range in terms of energy losses and life cycle. The results have shown that the estimation of the incoming solar energy in next parking phase produces a more efficient energy management, with reduction in fuel consumption, particularly at higher insolation. Some preliminary results have also shown that these benefits tend to increase if more irregular driving schedules are considered. Further studies is in course to analyze these aspects, as well as the effects of different latitudes and locations on the results.

The estimation of solar radiation could be accomplished on-board, by proper use of solar calculations based on a GPS module, of on line weather forecast and of correlations

between cloud cover and solar insolation (Nielsen et al., 1981). These aspects will be studied in the future developments of this work.

## REFERENCES

- André, M., Hammarström, U., Reynaud, I. (1999). Driving statistics for the assessment of air pollutant emissions from road transport. INRETS report, LTE9906, Bron, France, page 111, <http://www.inrets.fr/infos/cost319/index.html>.
- Arsie, I., Rizzo, G., Sorrentino, M. (2010). Effects of engine thermal transients on the energy management of series hybrid solar vehicles. *Control Engineering Practice*, doi:10.1016/j.conengprac.2010.01.015
- Arsie, I., Rizzo, G., Sorrentino, M. (2009). Genetic Algorithms Based Optimization of Intermittent ICE scheduling on a Hybrid Solar Vehicle. Proc. of European Control Conference 2009, ECC09, Budapest, August 23-26, 2009.
- Arsie, I., Rizzo, G., Sorrentino, M. (2007). Optimal Design and Dynamic Simulation of a Hybrid Solar Vehicle. *SAE Transactions - Journal of Engines*, Vol. 115-3, pp. 805-811.
- Arsie, I., Rizzo, G., Sorrentino, M. (2008). A Model for the Optimal Design of a Hybrid Solar Vehicle. *Review of Automotive Engineering*, Vol. 29:3, pp. 439-447.
- Buchmann, I. (2009). How to restore and prolong lead-acid batteries. <http://www.batteryuniversity.com/print-parttwo-35.htm>.
- Coraggio, G., Pisanti, C., Rizzo, G., Senatore, A. (2010). A moving solar roof for a hybrid solar vehicle. Accepted for publication on the proc. of IFAC Symposium Advances in Automotive Control 2010, July 12-14. Munich, Germany.
- Letendre, S., Perez, R., Herig, C. (2003). Vehicle Integrated PV: A Clean and Secure Fuel for Hybrid Electric Vehicles. Proc. of the American Solar Energy Society Solar 2003 Conference, June 21-23, 2003, Austin, TX-USA.
- Marano, V., Tulpule, P., Stockar, S., Onori, S., Rizzoni, G. (2009). Comparative study of different control strategies for Plug-In Hybrid Electric Vehicles. SAE Paper 2009-24-0071, 9th International Conference on Engines and Vehicles (ICE 2009), Sep 13-18, 2009, Capri (Italy).
- Nielsen, L., Prahm, L., Berkowicz, R., Conradsen, K. (1981). Net incoming radiation estimated from hourly global radiation and/or cloud observations. *J. Climatol.* Vol. 1, pp. 255-272.
- PVWatts (2009). <http://www.nrel.gov/rredc/pvwatts/>
- Rizzo, G., Sorrentino, M., Arsie, I. (2010). Rule-Based Optimization of Intermittent ICE Scheduling on a Hybrid Solar Vehicle. SAE paper 2009-24-0067, Proc. of ICE2009 9th International Conference on Engines & Vehicles, Capri, Italy, 13-18 September.
- Sorrentino, M., Arsie, I., Di Martino, R., Rizzo, G. (2010). On the Use of Genetic Algorithm to Optimize the On-Board Energy Management of a Hybrid Solar Vehicle. *Oil & Gas Science and Technology - Rev. IFP*, Vol. 65, No. 1, pp. 133-143.
- Sorrentino, M., Rizzo, G., Arsie, I. (2009). Analysis of Rule-Based Control Strategies for On-Board Energy Management of Hybrid Solar Vehicles. Proc. of E-COSM'09, the 2009 IFAC Workshop on Engine and Powertrain Control, Simulation and Modeling. Rueil-Malmaison, France, November 30-December 2, 2009.